Biochimica et Biophysica Acta 1843 (2014) 2079–2088

Contents lists available at ScienceDirect

Biochimica et Biophysica Acta

journal homepage: www.elsevier.com/locate/bbamcr

Nuclear distribution of claudin-2 increases cell proliferation in human lung adenocarcinoma cells

Akira Ikari [a,b,*], Ryo Watanabe [b], Tomonari Sato [b], Saeko Taga [a], Shun Shimobaba [a], Masahiko Yamaguchi [b], Yasuhiro Yamazaki [b], Satoshi Endo [a], Toshiyuki Matsunaga [a], Junko Sugatani [b]

[a] Laboratory of Biochemistry, Department of Biopharmaceutical Sciences, Gifu Pharmaceutical University, Gifu, Japan
[b] School of Pharmaceutical Sciences, University of Shizuoka, Shizuoka, Japan

ARTICLE INFO

Article history:
Received 13 January 2014
Received in revised form 2 May 2014
Accepted 29 May 2014
Available online 4 June 2014

Keywords:
Adenocarcinoma
Claudin-2
Cell proliferation
Nuclear distribution

ABSTRACT

Claudin-2 is expressed in human lung adenocarcinoma tissue and cell lines, although it is absent in normal lung tissue. However, the role of claudin-2 in cell proliferation and the regulatory mechanism of intracellular distribution remain undefined. Proliferation of human adenocarcinoma A549 cells was decreased by claudin-2 knockdown together with a decrease in the percentage of S phase cells. This knockdown decreased the expression levels of ZONAB and cell cycle regulators. Claudin-2 was distributed in the nucleus in human adenocarcinoma tissues and proliferating A549 cells. The nuclear distribution of ZONAB and percentage of S phase cells were higher in cells exogenously expressing claudin-2 with a nuclear localization signal than in cells expressing claudin-2 with a nuclear export signal. Nuclear claudin-2 formed a complex with ZO-1, ZONAB, and cyclin D1. Nuclear distribution of S208A mutant, a dephosphorylated form of claudin-2, was higher than that of wild type. We suggest that nuclear distribution of claudin-2 is up-regulated by dephosphorylation and claudin-2 serves to retain ZONAB and cyclin D1 in the nucleus, resulting in the enhancement of cell proliferation in lung adenocarcinoma cells.

1. Introduction

Lung cancer is one of the leading causes of cancer-related deaths, and its incidence is increasing all over the world. Non-small cell lung cancer (NSCLC) comprises over 80% of lung cancers diagnosed and has poor survival with a 5-year survival rate of 15% [1]. The long-term survival rate of patients with NSCLC remains unsatisfactory due to an unclear pathological mechanism. NSCLC includes two major histological subtypes: lung adenocarcinomas and squamous cell carcinomas. Adenocarcinomas are the most common type in the United States and Asia [2]. Tumor cells have the basic characteristics of unlimited proliferation, invasion, and metastasis. Cell–cell adhesion is important in maintaining epithelial morphology, cell proliferation, and migration [3].

At the apical pole of the intercellular junction of the lateral membrane, epithelial cells form the tight junctions (TJs), which compose a large complex of proteins including integral membrane proteins and cytoplasmic plaque proteins [4]. The TJs separate apical and basolateral epithelial compartments and limit the free diffusion of solutes across these compartments. Furthermore, some tight junctional proteins were shown to be involved in the regulation of cell proliferation [5,6]. Claudins and occludin are tetraspanning proteins that extend their extracellular loops across neighboring cells. The carboxy terminus of most claudins has a PDZ-binding motif that can interact with the PDZ domains of scaffolding proteins including zonula occludens (ZO)-1, -2, and -3 [7]. Claudins comprise a large family of 27 members that form homo- and heterotypic associations with each other [8,9]. Different combinations of claudins can confer different properties to epithelial cells in terms of physiological and pathophysiological functions.

Several claudins have been reported to exhibit abnormal expression in human cancers. For example, claudin-1 is down-regulated in breast cancer [10], whereas it is up-regulated in colon carcinoma [11] and melanoma [12]. Claudin-4 is up-regulated in pancreas [13] and biliary tract [14] cancers. Normal lung epithelia express claudin-1, -3, -4, -5, -7, and -18 [15,16]. In contrast, the expression of claudin-2 is high in adenocarcinomas [17]. Claudin-2 expression may be useful in a differential diagnosis and as a target of chemotherapy against lung adenocarcinoma. Recently, we revealed that claudin-2 is up-regulated by activation of a MEK/ERK/c-Fos pathway in human lung adenocarcinoma A549 cells [17]. However, the pathophysiological function of claudin-2 has not been fully elucidated in A549 cells.

ZO-1 associated nucleic acid binding protein (ZONAB) is a Y-box transcription factor that suppresses cell proliferation mediated by its interaction with the SH3 domain of ZO-1 in highly confluent epithelial

Abbreviations: ZONAB, ZO-1 associated nucleic acid binding protein; NSCLC, non-small cell lung cancer; TJs, tight junctions

* Corresponding author at: Laboratory of Biochemistry, Department of Biopharmaceutical Sciences, Gifu Pharmaceutical University, 1-25-4 Daigaku-nishi, Gifu 501–1196, Japan. Tel./fax: +81 58 230 8124.
E-mail address: ikari@gifu-pu.ac.jp (A. Ikari).

http://dx.doi.org/10.1016/j.bbamcr.2014.05.017
0167-4889/

cells [18]. In contrast, ZONAB is accumulated in the nucleus and up-regulates the expression of cell cycle regulators such as cyclin D1 and proliferating cell nuclear antigen in proliferating cells. ZONAB is overexpressed in several cancer tissues including the liver [19], pancreas [20], and colon [21]. The nuclear accumulation of ZONAB may be involved in the abnormal proliferation of cancer cells.

In the present study, we found that claudin-2 is distributed in the nucleus of human lung adenocarcinoma tissue and in both the nucleus and TJs of proliferating A549 cells. The introduction of claudin-2 siRNA decreased nuclear levels of ZONAB and cell cycle regulators, resulting in the suppression of G1/S cell cycle progression. The exogenous expression of claudin-2 with nuclear localization signal increased nuclear ZONAB levels and G1/S cell cycle progression in the endogenous claudin-2 knockdown cells. Claudin-2 formed a complex with ZO-1, ZONAB, and cyclin D1 in the nucleus. Nuclear distribution of claudin-2 was increased by dephosphorylation of Ser208. Our results indicate that claudin-2 may be abnormally distributed in the nucleus mediated by its dephosphorylation and enhances cell proliferation in lung adenocarcinoma.

2. Materials and methods

2.1. Materials

Rabbit anti-claudin-1, claudin-2, and ZO-1, goat anti-occludin, and mouse anti-claudin-2, and ZO-1 antibodies were obtained from Zymed Laboratories (South San Francisco, CA, USA). Unless otherwise indicated, rabbit anti-claudin-2 and mouse anti-ZO-1 antibodies were used in immunoblotting and immunofluorescence staining. Mouse anti-E-cadherin and nucleoporin p62 antibodies were from Becton Dickinson Biosciences (San Jose, CA, USA), rabbit anti-cyclin E1, mouse anti-Na^+/K^+-ATPase α subunit, and goat anti-β-actin antibodies were from Santa Cruz Biotechnology (Santa Cruz, CA, USA), mouse anti-cyclin D1 antibody was from Lab Vision (Fremont, CA, USA), rabbit anti-ZONAB antibody was from Upstate Cell Signaling Solutions (Lake Placid, NY, USA), and rabbit anti-Rb and phosphorylated Rb (phosphor-Ser795) antibodies were from Signalway antibody (College Park, MD, USA). Lipofectamine 2000 was from Invitrogen (Carlsbad, CA, USA). 4′,6-Diamidino-2-phenylindole (DAPI) and 3,8-diamino-5-[3-(diethylmethylammonio)propyl]-6-phenylphenanthridinium diiodide (PI) were from Dojindo laboratories (Kumamoto, Japan). All other reagents were of the highest grade of purity available.

2.2. Plasmid constructs

Human claudin-2 cDNA was amplified by RT-PCR and subcloned into the vector pCMV-Tag2, containing the FLAG epitope (BD Biosciences Clontech, Mountain view, CA, USA). The oligonucleotides encoding the nuclear localization signal (NLS) or nuclear export signal (NES) were fused to the amino-terminus of FLAG-claudin-2. The primers used to generate NLS-claudin-2 and NES-claudin-2 are listed in Supplementary Table 1. PCR products were digested by both Nhe I and Sal I, and were then cloned into the pTRE2/hyg vector (BD Biosciences Clontech). The S208A mutant of claudin-2 was generated using QuickChange II site-directed mutagenesis kit (Agilent Technologies, Santa Clara, CA, USA). Sequence analysis was consigned to Bio Matrix Research (Chiba, Japan).

2.3. Cell culture and transfection

The human lung adenocarcinoma A549 cell line was obtained from the RIKEN BRC through the National Bio-Resource Project of the MEXT, Japan. Cells were grown in Dulbecco's modified Eagle's medium (Sigma-Aldrich, Saint Louis, MO, USA) supplemented with 5% fetal calf serum (HyClone, Logan, UT, USA), 0.07 mg/ml penicillin-G potassium, and 0.14 mg/ml streptomycin sulfate in a 5% CO_2 atmosphere at 37 °C. Cells were transiently transfected with wild type claudin-2/pCMV-Tag2, S208A claudin-2/pCMV-Tag2, NLS-claudin-2/pTRE2, or NEL-claudin-2/pTRE2 vector using Lipofectamine 2000. Cells stably expressing the claudin-2/pSingle-tTS-shRNA vector were cultured in the presence of 1 μg/ml doxycycline for the inducible knockdown of endogenous claudin-2 expression [22]. Cell growth was assessed by counting the number of viable cells using a Neubauer chamber.

2.4. RNA isolation and RT-PCR

Total RNA was isolated from A549 cells using TRI reagent (Sigma-Aldrich). Reverse transcription was carried out with M-MLV reverse transcriptase (Promega, Madison, WI, USA) and random primers. Single strand cDNA was amplified by PCR using GoTaq DNA polymerase under the following conditions: denaturation at 94 °C for 0.5 min, annealing at 54 °C for 0.5 min, and extension at 72 °C for 0.5 min; these steps were repeated for 30 cycles. The primers used to PCR are listed in Supplementary Table 1. Quantitative real time PCR was performed using FastStart Universal SYBR Green Master (Roche Diagnostics, Mannheim, Germany). The threshold cycle (ct) for each PCR product was calculated with the instrument's software, and ct values obtained for claudin-1, claudin-2, E-cadherin, and ZO-1 were normalized by subtracting the ct values obtained for β-actin. The resulting Δct values were then used to calculate the relative change in mRNA expression as a ratio (R) according to the equation $R = 2^{-(\Delta ct(\text{each time}) - \Delta ct(24\ h))}$.

2.5. SDS-polyacrylamide gel electrophoresis (SDS-PAGE) and immunoblotting

The preparation of cell lysates was performed as described previously [22]. Nuclear and cytoplasmic extracts were prepared using NE-PER nuclear and cytoplasmic extraction reagents (Thermo Fisher Scientific, Waltham, MA, USA) according to the manufacturer's instructions. Samples were applied to SDS-PAGE and blotted onto a PVDF membrane. Phos-tag SDS-PAGE was used to analyze phosphorylation states of claudin-2. The membrane was then incubated with each primary antibody (1:1000 dilution) at 4 °C for 16 h, followed by a peroxidase-conjugated secondary antibody (1:5000 dilution) at room temperature for 1 h. Finally, the blots were incubated in Pierce immunoblotting Substrate (Thermo Fisher Scientific) and exposed to film, or incubated in ECL Prime Western Blotting Detection System (GE healthcare UK Ltd., Buckinghamshire, England) and scanned with a C-DiGit Blot Scanner (LI-COR Biotechnology, Lincoln, NE, USA). Band density was quantified with Doc-It LS image analysis software (UVP, Upland, CA, USA).

2.6. Immunoprecipitation

Cells were lysed in a immunoprecipitation buffer containing 150 mM NaCl, 0.5 mM EDTA, 0.5% Triton X-100, 50 mM Tris–HCl (pH 7.4), a protease inhibitor cocktail (Sigma-Aldrich), and 1 mM phenylmethylsulfonyl fluoride. Cell lysates were incubated with anti-claudin-2 or ZONAB antibody and Protein G-sepharose (GE Healthcare UK Ltd.) or ExactaCruz (Santa Cruz Biotechnology) for 16 h at 4 °C with gentle rocking. A negative control was immunoprecipitated with rabbit IgG. After centrifugation at 6,000 ×*g* for 1 min, the pellet was washed three times with the immunoprecipitation buffer. The immune pellets were solubilized in a sample buffer for SDS-PAGE.

2.7. Immunofluorescence staining

Lung tumor tissue array was obtained from BioChain Institute (Newark, CA, USA). Tissue was fixed in formalin followed by embedded in paraffin. Tissue arrays are 6 μm in thickness and mounted on positively charged glass slides followed by stained with H & E to ensure the quality. The slide includes 15 sections prepared from patients with lung adenocarcinoma. After blocking with 5% bovine serum albumin for 1 h, the

sections were incubated with anti-claudin-2 and ZO-1 antibodies (1:100) for 16 h at 4 °C. They were then incubated with Alexa Fluor 488 and Alexa Fluor 568-conjugated antibodies (1:100) including DAPI for 1 h at room temperature. A549 cells were cultured on cover glasses. Cells were fixed with methanol for 10 min at −20 °C, then permeabilized with 0.2% Triton X-100 for 15 min. After blocking with 2% Block Ace (Dainippon Sumitomo Pharma, Osaka, Japan) for 30 min, cells were incubated with anti-claudin-1, claudin-2, E-cadherin, ZO-1, or ZONAB antibody (1:100) for 16 h at 4 °C. They were then incubated with Alexa Fluor 488 and Alexa Fluor 568-conjugated antibodies (1:100) including DAPI for 1 h at room temperature. Immunolabeled tissues and cells were visualized on an LSM 510 confocal microscope (Carl Zeiss Microscopy GmbH, Göttingen, Germany).

2.8. Flow cytometry

After fixation with 70% ethanol, cells were incubated with 0.2 mg/ml RNase at 37 °C for 30 min. Cells were then incubated with 20 μg/ml PI at room temperature for 30 min. Each sample was analyzed by a BD FACSCant II Flow Cytometer (BD Biosciences) and the percentage of cells in the G1, S, and G2/M phases of the cell cycle was analyzed.

2.9. Statistics

Results are presented as means ± S.E.M. Differences between groups were analyzed with a one-way analysis of variance, and corrections for multiple comparison were made using Tukey's multiple comparison test. Comparisons between two groups were made using the Student's *t* test. Significant differences were assumed at $P < 0.05$.

3. Results

3.1. Effect of the culture period on claudin-2 expression

We examined the relationship between culture period and change in the expression of junctional proteins in A549 adenocarcinoma cells. A549 cells were cultured for 24, 48, 72, and 96 h, and reached a confluent state over 72 h (Fig. 1A). Claudin-2 mRNA levels transiently increased at 48 h, and then returned to basal levels (Fig. 1B and C). Similarly, its protein levels transiently increased at 48 and 72 h, and then returned to basal levels (Fig. 1B and D). In contrast, protein levels of claudin-1 and ZO-1 were stable for 96 h. The mRNA levels of E-cadherin increased at 72 and 96 h, while no significant change was observed in the protein levels. These results indicate that the expression levels of claudin-2 increase in proliferating cells.

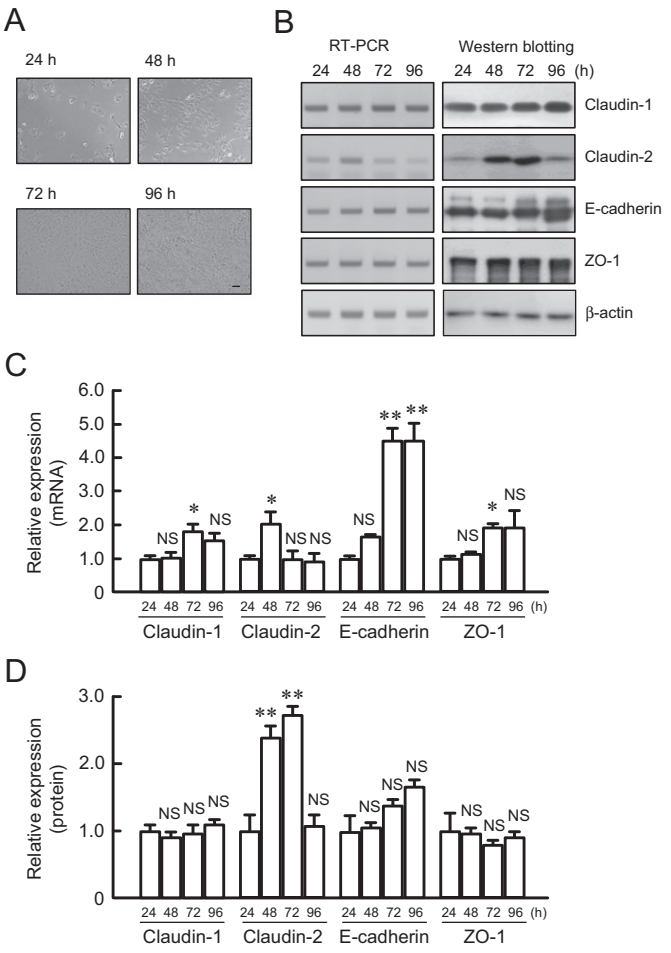

Fig. 1. Effect of the culture period on claudin-2 expression in A549 cells. (A) Representative images of cells from the light microscope were acquired 24, 48, 72, and 96 h post-seeding. Scale bar indicates 10 μm. (B) Left and right images show RT-PCR and immunoblotting, respectively. Total RNA and cell lysates were prepared from A549 cells cultured for 24, 48, 72, and 96 h post-seeding. RT-PCR was performed using primers for human claudin-1, claudin-2, E-cadherin, ZO-1, and β-actin. Cell lysates were immunoblotted with anti-claudin-1, claudin-2, E-cadherin, ZO-1, and β-actin antibodies. (C) The expression levels of mRNA were quantified by real-time PCR and were represented relative to values at 24 h. (D) The expression levels of protein were represented relative to values at 24 h. $^{*}P < 0.05$ and $^{**}P < 0.01$ significantly different from 24 h. NS, $P > 0.05$. $n = 3$.

3.2. Inhibition of cell proliferation by the knockdown of claudin-2

To examine the effect of claudin-2 expression on cell proliferation, we established knockdown cells of claudin-2 using an inducible shRNA vector [22]. Claudin-2 shRNA decreased claudin-2 protein levels by 64.1% ($n = 3$). Cell numbers were counted 24, 48, and 72 h post-seeding. Cell numbers were significantly decreased by the knockdown of claudin-2 at 48 and 72 h (Fig. 2A). Cell cycle progression affects cell proliferation. Therefore, we examined the effect of knocking down claudin-2 expression on cell cycle progression. The percentage of cells in the S phase was significantly decreased by claudin-2 knockdown, whereas that in the G1 phase was increased (Fig. 2B). The percentage of cells in G2/M was unchanged. The decrease in claudin-2 expression by U0126, a MEK inhibitor, causes the decrease in the percentage of cells in the S phase and increase in that in the G1 phase (Fig. S1). These results suggest that claudin-2 expression affects cell cycle progression from G1 to S phases. In the G1 to S phase transition, the activity of cyclin-dependent kinases (CDKs) is positively regulated by cyclin D1 and E1 [23,24]. Rb is phosphorylated by complexes of cyclins and CDKs, leading to entry into S phase. The knockdown of cyclin D1 by siRNA is reported to decrease cell proliferation in A549 cells [25]. The expression levels of cyclin D1, cyclin E1, and phosphorylated Rb were significantly decreased by the knockdown of claudin-2 (Fig. 2C and D). These results indicate that claudin-2 increases the expression of cell cycle regulators, resulting in the acceleration of the G1–S transition.

3.3. Decrease in the nuclear distribution of ZONAB by claudin-2 knockdown

Immunofluorescence measurements showed that ZONAB is distributed in both the nucleus and cytoplasm, whereas claudin-2 distributed in both the nucleus and cell–cell border area (Fig. 3A). Claudin-2 knockdown decreased the red signal of claudin-2 and the nuclear green signal of ZONAB. Similarly, immunoblotting analysis showed that the nuclear distribution of ZONAB is significantly decreased by claudin-2 knockdown (Fig. 3B and C). The cytoplasmic distribution of ZONAB was increased by claudin-2 knockdown, but this change was not significant. These results indicate that claudin-2 increases the nuclear levels of ZONAB.

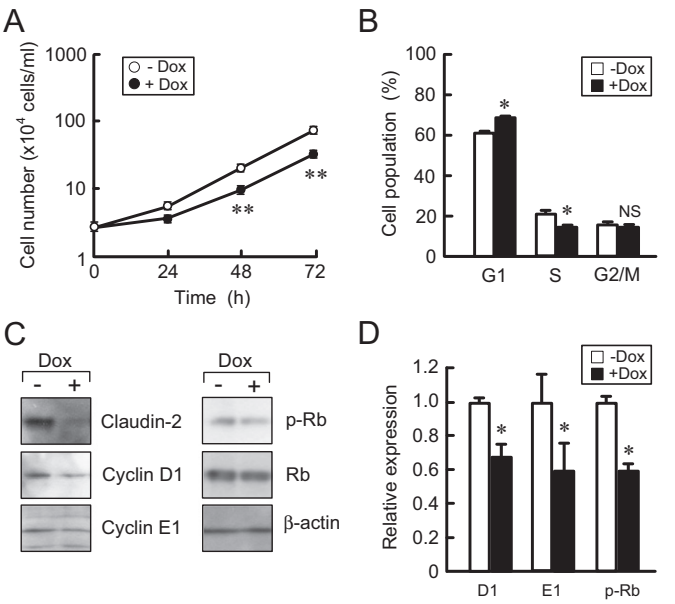

Fig. 2. Effect of claudin-2 knockdown on cell proliferation and cell cycle regulators. Cells expressing the claudin-2/pSingle-tTS-shRNA vector were cultured in the presence and absence of 1 μg/ml doxycycline for 24, 48, and 72 h (A) or 72 h (B–D). (A) After detaching with trypsin, the viable cell number was counted. (B) The percentage in the G1, S, and G2/M phases was analyzed by a flow cytometer. (C) Total cell lysate was immunoblotted with anti-claudin-2, cyclin D1, cyclin E1, Rb, phosphorylated Rb (p-Rb) and β-actin antibodies. (D) The expression levels of cyclin D1, cyclin E1, and p-Rb were represented relative to values in the absence of doxycycline. $^*P < 0.05$ significantly different from - Dox. NS, $P > 0.05$. $n = 3$.

3.4. Decrease in cell cycle progression by ZONAB knockdown

To examine the effect of ZONAB expression on cell cycle progression, we knocked down ZONAB expression using siRNA. ZONAB siRNA significantly decreased ZONAB protein levels by 59.6% (Fig. 4A and B). Similar to the knockdown of claudin-2, the expression levels of cyclin D1, cyclin E1, and phosphorylated Rb were decreased by ZONAB knockdown. Furthermore, the percentage of cells in the S phase was significantly decreased by ZONAB knockdown, whereas that in the G1 phase was increased (Fig. 4C). These results indicate that the decrease in ZONAB expression affects the expression levels of cyclin D1, cyclin E1, and phosphorylated Rb, resulting in the suppression of the G1–S transition.

3.5. Nuclear distribution of tight junctional protein claudin-2

The intracellular distribution of claudin-2 was examined by immunocytochemistry. At 24 h post-seeding, claudin-2 was distributed in the nucleus, cytoplasm, and cell–cell border area (Fig. 5A). The milder detergent, digitonin, is able to selectively permeabilize the plasma membrane. Claudin-2 was detected in the nucleus in Triton X-100-permeabilized cells, whereas it was not detected in the nucleus in digitonin-permeabilized cells (Fig. S2). These results suggest that claudin-2 is not distributed in an outer nuclear membrane. ZO-1 and E-cadherin were distributed in the nucleus, cytoplasm, and cell–cell border area. Claudin-1 was mainly distributed in the cell–cell border area and was partly distributed in the nucleus and cytoplasm. At 72 h post-seeding, claudin-1 and E-cadherin were mainly distributed in the cell–cell border area, whereas claudin-2 was distributed in both the nucleus and cell–cell border area (Fig. 5B). Similar results were observed in immunoblotting analysis using nuclear and cytoplasmic extracts (Fig. 6). The isolation of nuclear and cytoplasmic fractions was checked by nucleoporin p62, a nuclear protein, and Na^+/K^+-ATPase, a cytoplasmic protein, respectively. Expression levels of claudin-2 and ZO-1 in both the nuclear and cytoplasmic fractions significantly increased at 72 h, and then returned to basal levels. The distribution of claudin-2

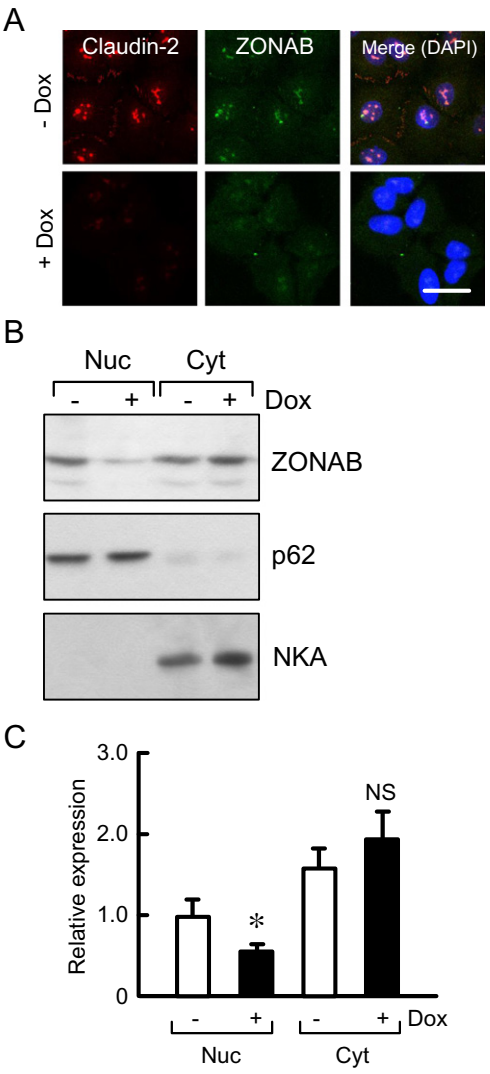

Fig. 3. Decrease in nuclear ZONAB expression by claudin-2 knockdown. Cells expressing the claudin-2/pSingle-tTS-shRNA vector were cultured in the presence and absence of 1 μg/ml doxycycline for 72 h. (A) Cells were stained with claudin-2 (red), ZONAB (green), and DAPI (blue). The scale bar represents 10 μm. (B) Nuclear (Nuc) and cytoplasmic (Cyt) fractions were immunoblotted with anti-ZONAB, nucleoporin p62, and Na^+/K^+-ATPase α subunit (NKA) antibodies. (C) The expression levels of ZONAB were represented relative to values in the cytoplasmic fractions in the absence of doxycycline. $^*P < 0.05$ significantly different from - Dox. NS, $P > 0.05$. $n = 3$.

and ZO-1 in both the nucleus and cytosol was checked by another mouse anti-claudin-2 and rabbit anti-ZO-1 antibodies (Fig. S3). Unlike claudin-2, cytoplasmic claudin-1 levels increased in a time-dependent manner and nuclear claudin-1 levels remained constant for 96 h. These results indicate that claudin-2 and ZO-1 are distributed in both the nucleus and TJs, and the expression levels of these proteins peaked at 72 h in proliferating cells.

3.6. Increase in claudin-2 expression in human lung adenocarcinoma tissue

We found that claudin-2 is distributed in both the nucleus and TJs of A549 cells, but its distribution in human adenocarcinoma tissue remains undefined. Therefore, the localization of claudin-2 and ZO-1, a scaffolding protein of the TJ, was examined using human lung tumor tissue array. Claudin-2 protein was expressed in lung adenocarcinoma tissue and was co-localized with ZO-1 in the nuclear area (Fig. 7). The nuclear co-localization of claudin-2 and ZO-1 is similar to those in A549 cells.

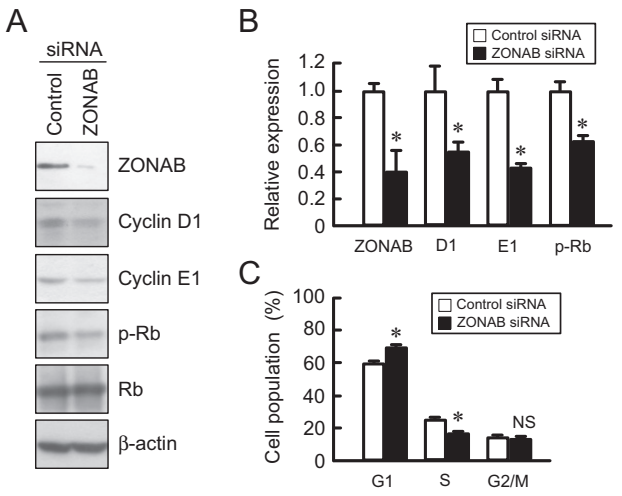

Fig. 4. Effect of ZONAB knockdown on cell cycle progression. Cells were transfected with negative control or ZONAB siRNA using Lipofectamine 2000. (A) Cell lysates were immunoblotted with anti-ZONAB, cyclin D1, cyclin E1, Rb, p-Rb and β-actin antibodies. (B) The expression levels of ZONAB, cyclin D1, cyclin E1, and p-Rb were represented relative to values in the presence of control siRNA. (C) The percentage in the G1, S, and G2/M phases was analyzed by a flow cytometer. $^{*}P < 0.05$ significantly different from control siRNA. NS, $P > 0.05$. $n = 3$.

3.7. Nuclear claudin-2 increased the G1–S transition

As shown in Fig. 2, claudin-2 knockdown decreased the percentage of cells in the S phase, whereas it increased it in the G1 phase. Increased claudin-2 expression was noted in the nucleus. However, it has not been investigated whether cell cycle progression is regulated by nuclear claudin-2. There is no report what sequence is involved in the nuclear distribution of claudin-2. We searched classical NLS sequences using nuclear localization software-based analysis (Nuclear Localization Signal database, http://rostlab.org/services/nlsdb/). However, no classical NLS sequences were detected in human claudin-2 sequence. Therefore, we examined the effects of NLS- and NES-claudin-2 expression on cell cycle progression. To avoid the effect of endogenous claudin-2, NLS- and NES-claudin-2 were transfected into claudin-2 knockdown cells. The exogenous expression of NLS- and NES-claudin-2 protein was confirmed by immunoblotting using FLAG and claudin-2 antibodies (Fig. 8A). Single band of claudin-2 was detected in control cells, whereas no band was detected in mock cells. The band of NLS- and NES-claudin-2 was detected above endogenous claudin-2. Immunofluorescence measurements and immunoblotting analysis showed that NLS-claudin-2 is distributed in the nucleus, whereas NES-claudin-2 was mainly distributed in the cytoplasm (Fig. 8A and B). The nuclear distribution of ZONAB was significantly increased by the expression of NLS-claudin-2 compared with that of NES-claudin-2 (Fig. 8C). Furthermore, the percentage of cells in the S phase and G1 phase were higher and lower, respectively, with NLS-claudin-2 than with NES-claudin-2 (Fig. 8D). These results indicate that nuclear claudin-2 increases the nuclear distribution of ZONAB, resulting in the acceleration of the G1–S transition.

3.8. Association of nuclear claudin-2 with ZONAB, ZO-1, and cyclin D1

Claudin-2, ZO-1, and ZONAB were distributed in the nucleus of proliferating cells, and the fluorescence pattern of claudin-2 was merged with those of ZO-1 and ZONAB (Figs. 3 and 5). Therefore, these results raised the possibility that claudin-2 is associated with ZO-1 and ZONAB in the nucleus. In the immunoprecipitation assay, nuclear claudin-2 was associated with ZO-1 and ZONAB (Fig. 9). Furthermore, claudin-2 was associated with cyclin D1, but not with cyclin E. These

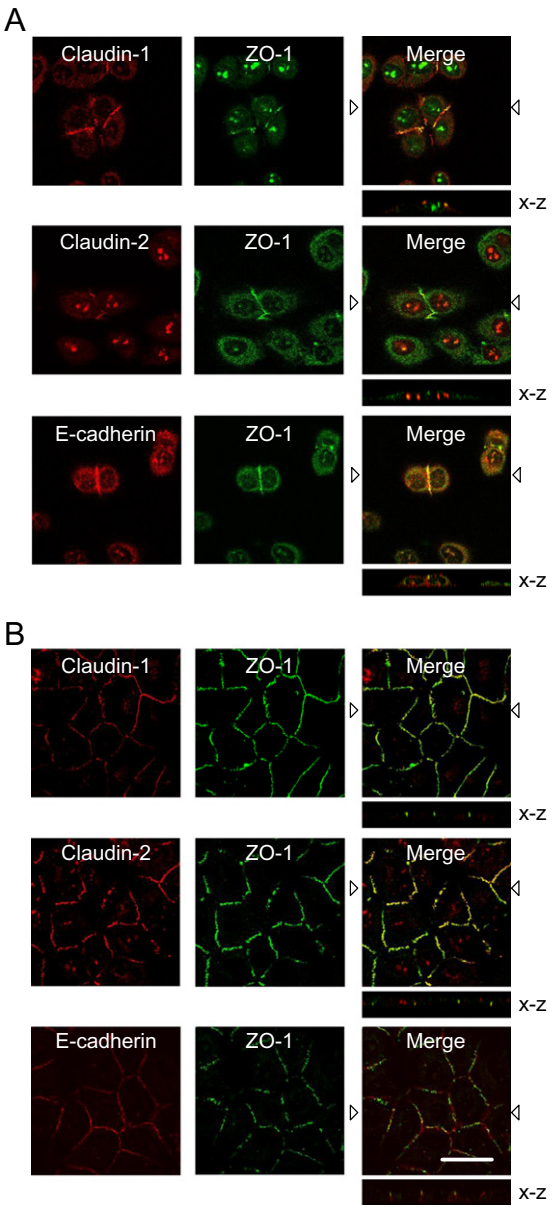

Fig. 5. Intracellular distribution of junctional proteins. Cells were cultured for 24 (A) or 72 h (B) and stained with anti-ZO-1 plus claudin-1, claudin-2, or E-cadherin antibody. The co-localization of these proteins appears yellow in the merged images. Lower panels (x–z) show the vertical sections indicated by the triangles at the merged images. The scale bar represents 10 μm.

results indicate that claudin-2 forms a complex with ZO-1, ZONAB, and cyclin D1 in the nucleus.

3.9. Increase in nuclear claudin-2 level by dephosphorylation

Claudin-2 was distributed in both the nucleus and TJs in A549 cells, but the underlying mechanism is not fully understood. PDZ binding domain in the carboxyl-terminal tail of claudins is necessary for the distribution in the TJs [26]. The ratio of nuclear claudin-2 in wild type was similar to that in ΔPDZ mutant (Fig. S4). In contrast, the ratio of nuclear claudin-2 in Δcytosol mutant was significantly lower than that in wild type. These results indicate that claudin-2 may have NLS sequence in the carboxyl-terminal cytosolic region and PDZ binding motif is not NLS sequence. Claudin-2 has recently been reported to be constitutively phosphorylated at S208 in mouse kidney and renal tubular MDCK II cells [27]. We examined the effect of phosphorylation on the nuclear

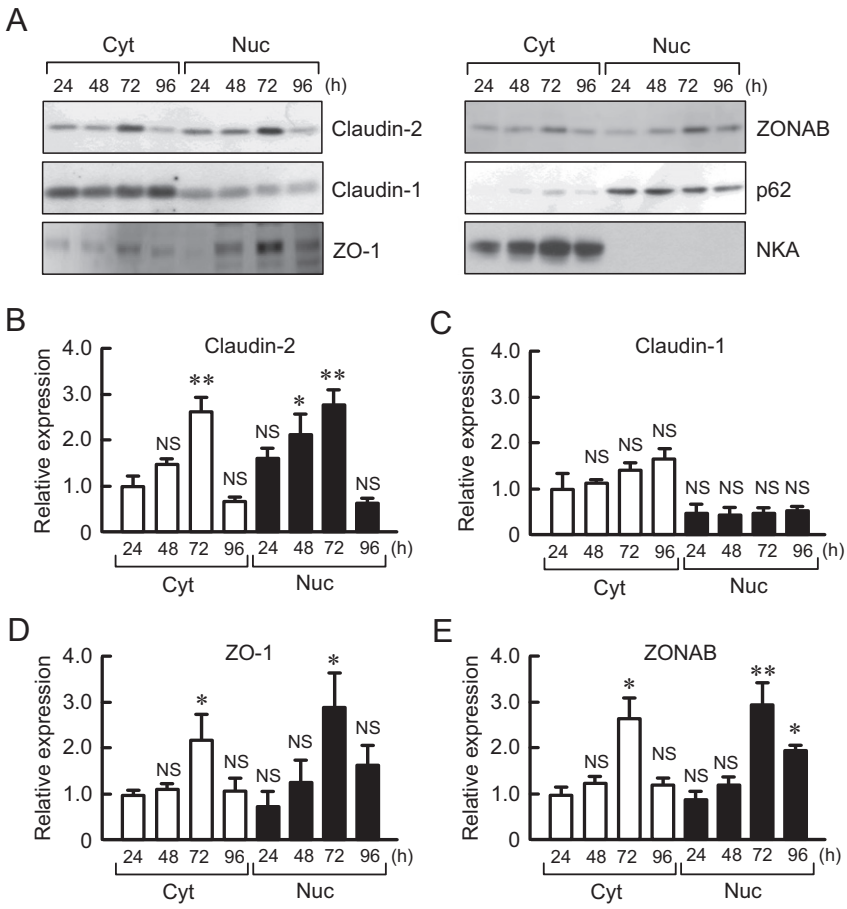

Fig. 6. Nuclear and cytoplasmic distribution of claudin-2. (A) Cells were cultured for 24, 48, 72, and 96 h. Nuclear (Nuc) and cytoplasmic (Cyt) fractions were immunoblotted with anti-claudin-1, claudin-2, ZO-1, ZONAB, nucleoporin p62, and NKA antibodies. (B and C) The expression levels of claudin-2 (B), claudin-1 (C), ZO-1 (D), and ZONAB (E) were represented relative to values at 24 h in the cytoplasmic fraction. $^{*}P < 0.05$ and $^{**}P < 0.01$ significantly different from values at 24 h in the cytoplasmic fraction. NS, $P > 0.05$. $n = 3$-4.

distribution of claudin-2. In a phos-tag gel, the upper band of claudin-2 detected in control cells was disappeared by forskolin, indicating forskolin dephosphorylates claudin-2 (Fig. 10). Forskolin increased nuclear distribution of claudin-2 compared to control. S208A mutant, a dephosphorylated form of claudin-2, was detected in lower band in a phos-tag gel (Fig. 11) similar to those in the forskolin-treated cells.

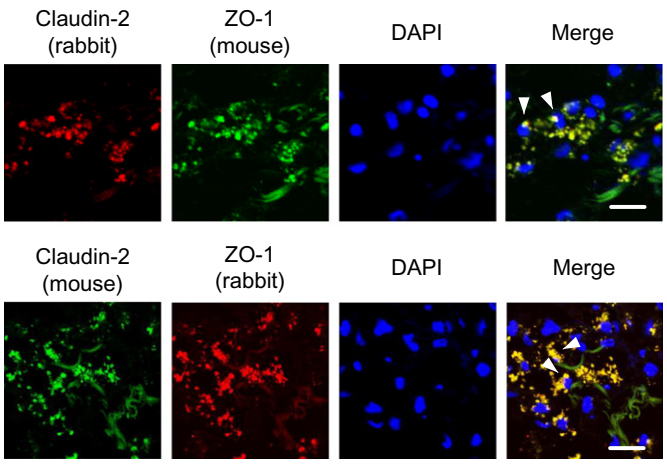

Fig. 7. Expression of claudin-2 in human lung adenocarcinoma tissue. The sections containing lung adenocarcinoma tissues were stained with two types of anti-claudin-2 and ZO-1 antibodies, and DAPI (blue). The arrowheads indicate the co-localization of claudin-2 with ZO-1 in the nucleus. The scale bar represents 10 μm.

The nuclear distribution of S208A was much more abundant than that of wild type. The association of claudin-2 with ZO-1, ZONAB, and cyclin D1 was increased by forskolin or mutation of S208A. These results suggest that dephosphorylation of Ser208 is involved in the nuclear distribution of claudin-2 and formation of the claudin-2 complex with ZO-1, ZONAB, and cyclin D1 in the nucleus.

4. Discussion

We recently reported that mRNA levels of claudin-2 are much more abundant in human lung adenocarcinoma tissue and adenocarcinoma cell lines including A549, RERF-LC-MA, and PC-3 than in normal lung tissue [17]. Similar to lung adenocarcinoma, claudin-2 expression is higher in colonic [28], gastric [29], breast [30], and cervical [31] cancers. In contrast, claudin-2 expression is down-regulated in breast carcinoma [32] and prostate adenocarcinoma [33]. These reports suggest that the increase in claudin-2 expression might be a consequence of carcinogenesis with organ specificity. Forced claudin-2 expression in colon cancer cells increases tumor growth [28], but the role of claudin-2 in cell proliferation has remained undefined in lung adenocarcinoma. In the present study, we showed that claudin-2 protein levels transiently increased at 48 and 72 h under proliferating conditions, and then returned to basal levels under resting confluent conditions (Fig. 1). Claudin-2 knockdown decreased the cell number and cell population in the S phase concomitant with the decrease in cyclin D1, cyclin E1, and phosphorylated Rb (Fig. 2). Claudin-2 may enhance cell proliferation mediated by the acceleration of cell cycle G1–S transition in A549 cells.

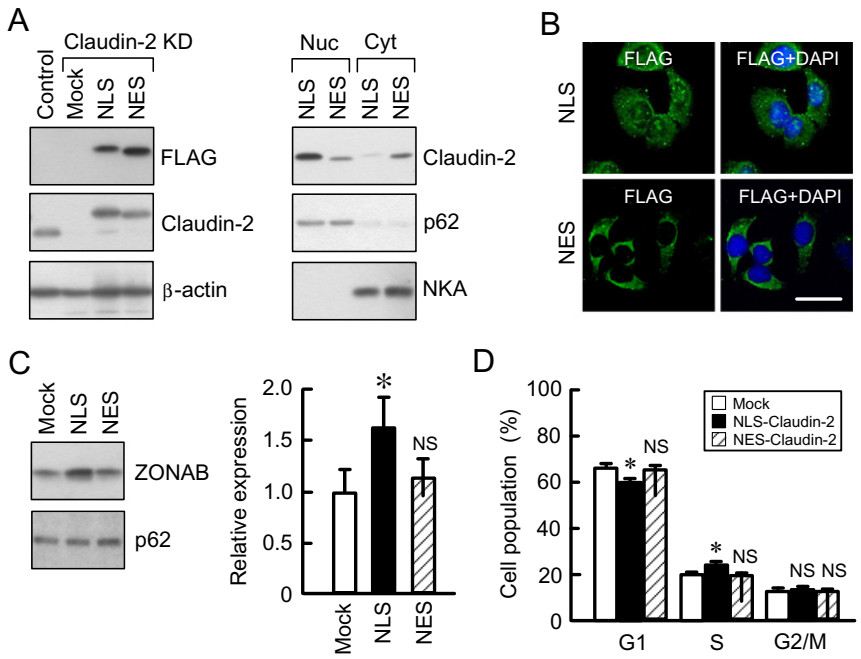

Fig. 8. Effects of NLS- and NES-claudin-2 expression on cell cycle progression. A mock, NLS-claudin-2, or NES-claudin-2 expression vector was transiently transfected into the cells expressing the claudin-2 shRNA/pSingle-tTS-shRNA vector. Cells were cultured in the presence (claudin-2 KD) of 1 μg/ml doxycycline without control. (A) Total cell lysate, nuclear (Nuc), and cytoplasmic (Cyt) fractions were immunoblotted with anti-FLAG, claudin-2, nucleoporin p62, NKA, or β-actin antibody. (B) Cells were stained with anti-FLAG antibody (green) and DAPI (blue). The scale bar represents 10 μm. (C) The nuclear fraction was immunoblotted with anti-ZONAB and nucleoporin p62 antibodies. The expression levels of nuclear ZONAB were represented relative to values in the cells transfected with NES-claudin-2. (D) The percentage in the G1, S, and G2/M phases was analyzed by a flow cytometer. $^{*}P < 0.05$ significantly different from mock. NS, $P > 0.05$. $n = 3$-4.

ZONAB can shuttle between the TJ and nucleus according to cell density [34]. A reduction in ZONAB in the nucleus is reported to reduce the proliferation of renal epithelial cells [35]. We found that ZONAB is highly distributed in the nucleus in the claudin-2-expressing A549 cells (Fig. 3). Claudin-2 knockdown decreased the nuclear distribution of ZONAB. Furthermore, ZONAB siRNA decreased the cell population in the S phase concomitant with the decrease in cyclin D1, cyclin E1, and phosphorylated Rb (Fig. 4). These results were similar to those in claudin-2 knockdown cells (Fig. 2). Claudin-2 may enhance cell proliferation mediated by the increase in the nuclear distribution of ZONAB in A549 cells.

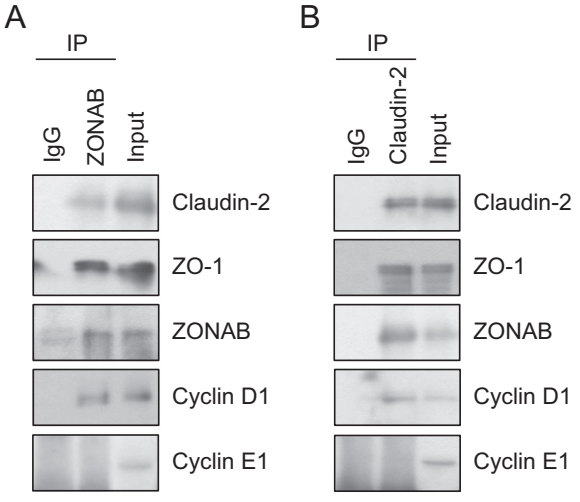

Fig. 9. Association of nuclear claudin-2 with ZO-1, ZONAB, and cyclin D1. Nuclear fractions were prepared from A549 cells cultured for 72 h. Aliquots were immunoprecipitated with anti-ZONAB (A) or claudin-2 (B) antibody. Negative controls were immunoprecipitated with rabbit IgG. Immune pellets were then immunoblotted with anti-claudin-2, ZO-1, ZONAB, cyclin D1, and cyclin E1 antibodies. $n = 3$.

The nuclear distribution of several cell junctional proteins including ZO-1, ZO-2, and ZONAB is known to be correlated with oncogenic transformation and cell proliferation [36,37]. It should be noted that both claudin-2 and ZO-1 are distributed in the nucleus in human lung adenocarcinoma tissue (Fig. 7). Immunofluorescence and immunoblotting analyses showed that claudin-2 is distributed in the nucleus of A549 cells under proliferating conditions (Figs. 5 and 6). The distribution of claudin-2 and ZO-1 in both the nucleus and cytosol was revealed by two types of claudin-2 and ZO-1 antibodies. We suggest that nuclear claudin-2 is involved in the up-regulation of cell proliferation in lung adenocarcinoma. The nuclear distribution of claudin-1 has been reported in several cancers. The pathophysiological function of nuclear claudin-1 remains to be determined, but nuclear claudin-1 may be associated with nuclear localization of β-catenin in colon cancer [11] and may reduce apoptosis of nasopharyngeal carcinoma cells under serum withdrawal of fluorouracil treatment [38]. Our results indicated that claudin-1 is mainly distributed in the TJ and cytoplasmic fraction in A549 cells. Furthermore, claudin-1 protein levels remained constant under proliferating and resting confluent conditions. We suggest that nuclear claudin-2, but not claudin-1, plays key role in enhancing cell proliferation in A549 cells.

Claudin-2 and ZO-1 were immunoprecipitated with ZONAB antibody (Fig. 9). In contrast, these proteins were not immunoprecipitated with rabbit IgG. Similarly, ZO-1 and ZONAB were immunoprecipitated with claudin-2 antibody. Cyclin D1 was immunoprecipitated with claudin-2 or ZONAB antibody, while cyclin E was not. Our results suggest that claudin-2 forms a complex with ZO-1, ZONAB, and cyclin D1 in the nucleus, resulting in the acceleration of cell cycle G1–S transition in A549 cells. The overexpression of cyclin D1 has been frequently found in NSCLC [39,40]. Cyclin D1 is phosphorylated by glycogen synthase kinase-3β and exported from the nucleus. Following its nuclear export, cyclin D1 is ubiquitinated by ubiquitin-ligases and degraded by the

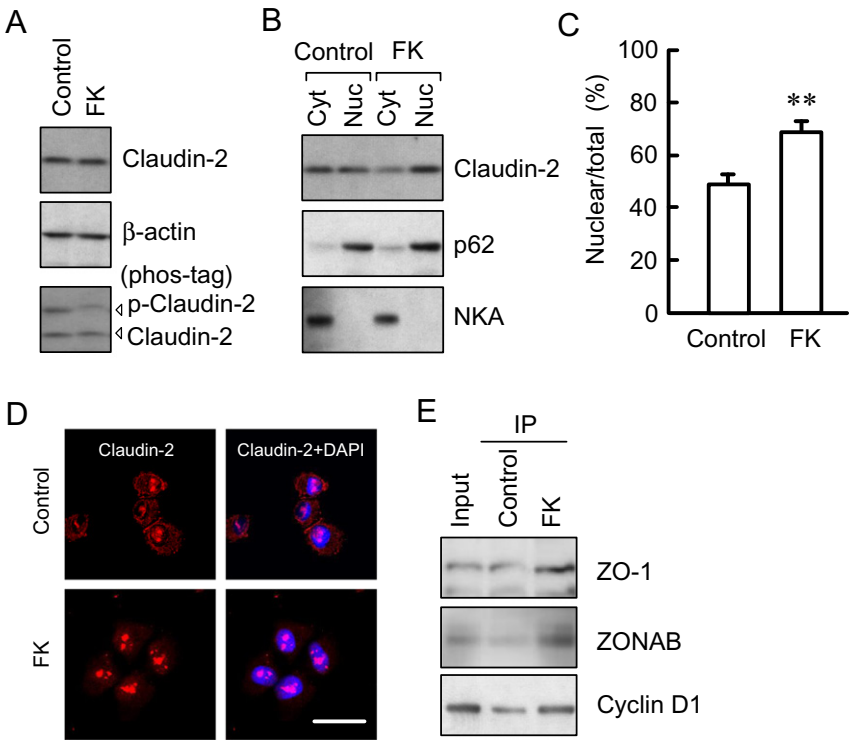

Fig. 10. Increase in nuclear distribution of claudin-2 by forskolin. (A) Cells were incubated with 10 μM forskolin for 2 h. Total cell lysates were applied on normal or phos-tag gels and immunoblotted with claudin-2 and β-actin antibodies. (B) Nuclear (Nuc) and cytoplasmic (Cyt) fractions were immunoblotted with anti-claudin-2, nucleoporin p62, and NKA antibodies. (C) The nuclear levels of claudin-2 were represented relative to the total level. (D) Cells were stained with anti-claudin-2 antibody (red) and DAPI (blue). The scale bar represents 10 μm. (E) Nuclear fractions were prepared from control and forskolin-treated A549 cells. Aliquots were immunoprecipitated with anti-claudin-2 antibody. Immune pellets were then immunoblotted with anti-ZO-1, ZONAB, and cyclin D1 antibodies. $^{**}P < 0.01$ significantly different from values of control. $n = 4$.

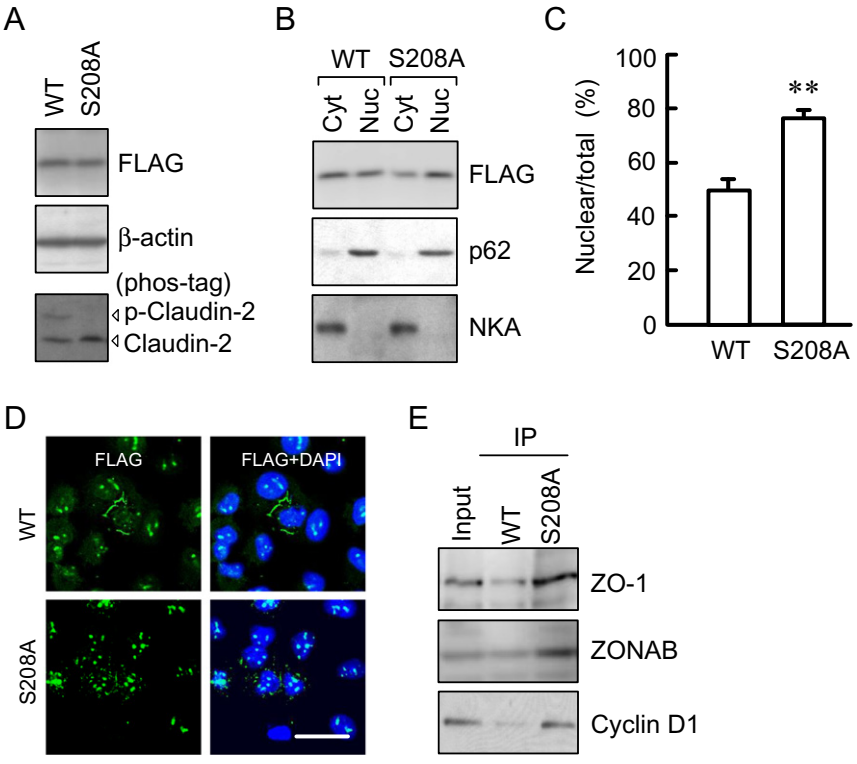

Fig. 11. Nuclear distribution of wild type and S208A claudin-2. Wild type (WT) and S208A claudin-2 expression vector was transiently transfected into the cells. (A) Total cell lysates were applied on normal or phos-tag gels and immunoblotted with anti-FLAG and β-actin antibodies. (B) Nuclear (Nuc) and cytoplasmic (Cyt) fractions were immunoblotted with anti-FLAG, nucleoporin p62, and NKA antibodies. (C) The nuclear levels of FLAG-tagged claudin-2 were represented relative to the total level. (D) Cells were stained with anti-FLAG antibody (green) and DAPI (blue). The scale bar represents 10 μm. (E) Nuclear fractions were prepared from the cells transfected with WT and S208 claudin-2. Aliquots were immunoprecipitated with anti-FLAG antibody. Immune pellets were then immunoblotted with anti-ZO-1, ZONAB, and cyclin D1 antibodies. $^{**}P < 0.01$ significantly different from values of WT. $n = 3$.

proteasome [41,42]. The complex of claudin-2 with ZO-1, ZONAB, and cyclin D1 may prevent the phosphorylation or nuclear export of cyclin D1.

Claudin-2 knockdown decreased cell proliferation in A549 cells. Does nuclear claudin-2 play a role in the regulation of cell growth? Unfortunately, we could not detect any classical NLS sequences using nuclear localization software-based analysis. Lange et al. [43] reported that about 57% of steady-state nuclear proteins contain classical NLS, whereas about 43% do not using a global yeast GFP screen. The nuclear distribution of ZONAB and percentage of the S phase were higher with NLS-claudin-2 than with NES-claudin-2, indicating that nuclear claudin-2 is involved in the promotion of cell cycle progression. This is the first report to show that nuclear claudin-2 can function as a positive regulator of cell proliferation.

Forskolin and prostaglandin E_2 decrease the level of phosphorylated claudin-2 in MDCK II cells [27]. They suggest that the increase in cAMP may activate a protein phosphatase that dephosphorylates claudin-2 at S208. The cytoplasmic distribution of S208A mutant, a non-phosphorylatable form of claudin-2, is much more abundant than that of wild type. Phosphorylation of S208 may play a major role in the retention of claudin-2 at the plasma membrane. Similar to the report in MDCK II cells, claudin-2 was phosphorylated in A549 cells and forskolin decreased the level of phosphorylated claudin-2 (Fig. 10). The nuclear distribution of claudin-2 in forskolin-treated cells (Fig. 10) and S208A mutant (Fig. 11) was much more abundant than that of claudin-2 in control cells and wild type, respectively. We suggest that nuclear transport or retention of claudin-2 is partially regulated by phosphorylation at S208.

Taken together, claudin-2 was distributed in the nucleus and TJs in human lung adenocarcinoma tissue and A549 cells. Claudin-2 knockdown decreased the nuclear distribution of ZONAB and suppressed cell cycle G1–S transition. Nuclear claudin-2 formed a complex with ZO-1, ZONAB, and cyclin D1, and enhances cell proliferation. We suggest that nuclear claudin-2 expression is involved in the progression of lung adenocarcinoma. Nuclear claudin-2 may be a novel target for the development of anticancer agents.

Supplementary data to this article can be found online at http://dx.doi.org/10.1016/j.bbamcr.2014.05.017.

Author contributions

R.W., T.S., S.T., and S.S. performed experiments and analyzed the data. M.Y., Y.Y., and J.S. contributed to the experimental plan and discussion of the manuscript. S.E. and T.M. contributed to the discussion of the manuscript. A.I. contributed to supervision of the project, interpretation of the data and writing the paper.

Acknowledgements

This work was supported in part by a Grant-in-Aid for Scientific Research (C) from the JSPS KAKENHI (23590263) and by grants from the Pharmacological Research Foundation, Tokyo, Takeda Science Foundation, and SRI academic research grant (to A.I.).

References

[1] G.V. Scagliotti, P. Parikh, J. von Pawel, B. Biesma, J. Vansteenkiste, C. Manegold, P. Serwatowski, U. Gatzemeier, R. Digumarti, M. Zukin, J.S. Lee, A. Mellemgaard, K. Park, S. Patil, J. Rolski, T. Goksel, F. de Marinis, L. Simms, K.P. Sugarman, D. Gandara, Phase III study comparing cisplatin plus gemcitabine with cisplatin plus pemetrexed in chemotherapy-naive patients with advanced-stage non-small-cell lung cancer, J. Clin. Oncol. 26 (2008) 3543–3551.
[2] N. Shivapurkar, J. Reddy, P.M. Chaudhary, A.F. Gazdar, Apoptosis and lung cancer: a review, J. Cell. Biochem. 88 (2003) 885–898.
[3] V.M. Braga, Cell–cell adhesion and signalling, Curr. Opin. Cell Biol. 14 (2002) 546–556.
[4] S. Tsukita, M. Furuse, M. Itoh, Multifunctional strands in tight junctions, Nat. Rev. Mol. Cell Biol. 2 (2001) 285–293.
[5] S. Tsukita, Y. Yamazaki, T. Katsuno, A. Tamura, Tight junction-based epithelial microenvironment and cell proliferation, Oncogene 27 (2008) 6930–6938.
[6] K. Matter, S. Aijaz, A. Tsapara, M.S. Balda, Mammalian tight junctions in the regulation of epithelial differentiation and proliferation, Curr. Opin. Cell Biol. 17 (2005) 453–458.
[7] M. Itoh, M. Furuse, K. Morita, K. Kubota, M. Saitou, S. Tsukita, Direct binding of three tight junction-associated MAGUKs, ZO-1, ZO-2, and ZO-3, with the COOH termini of claudins, J. Cell Biol. 147 (1999) 1351–1363.
[8] K. Mineta, Y. Yamamoto, Y. Yamazaki, H. Tanaka, Y. Tada, K. Saito, A. Tamura, M. Igarashi, T. Endo, K. Takeuchi, S. Tsukita, Predicted expansion of the claudin multigene family, FEBS Lett. 585 (2011) 606–612.
[9] K. Turksen, T.C. Troy, Barriers built on claudins, J. Cell Sci. 117 (2004) 2435–2447.
[10] F. Kramer, K. White, M. Kubbies, K. Swisshelm, B.H. Weber, Genomic organization of claudin-1 and its assessment in hereditary and sporadic breast cancer, Hum. Genet. 107 (2000) 249–256.
[11] P. Dhawan, A.B. Singh, N.G. Deane, Y. No, S.R. Shiou, C. Schmidt, J. Neff, M.K. Washington, R.D. Beauchamp, Claudin-1 regulates cellular transformation and metastatic behavior in colon cancer, J. Clin. Invest. 115 (2005) 1765–1776.
[12] P.D. Leotlela, M.S. Wade, P.H. Duray, M.J. Rhode, H.F. Brown, D.T. Rosenthal, S.K. Dissanayake, R. Earley, F.E. Indig, B.J. Nickoloff, D.D. Taub, O.P. Kallioniemi, P. Meltzer, P.J. Morin, A.T. Weeraratna, Claudin-1 overexpression in melanoma is regulated by PKC and contributes to melanoma cell motility, Oncogene 26 (2007) 3846–3856.
[13] L.S. Nichols, R. Ashfaq, C.A. Iacobuzio-Donahue, Claudin 4 protein expression in primary and metastatic pancreatic cancer: support for use as a therapeutic target, Am. J. Clin. Pathol. 121 (2004) 226–230.
[14] C. Lodi, E. Szabo, A. Holczbauer, E. Batmunkh, A. Szijarto, P. Kupcsulik, I. Kovalszky, S. Paku, G. Illyes, A. Kiss, Z. Schaff, Claudin-4 differentiates biliary tract cancers from hepatocellular carcinomas, Mod. Pathol. 19 (2006) 460–469.
[15] C.B. Coyne, T.M. Gambling, R.C. Boucher, J.L. Carson, L.G. Johnson, Role of claudin interactions in airway tight junctional permeability, Am. J. Physiol. Lung Cell. Mol. Physiol. 285 (2003) L1166–L1178.
[16] B.L. Daugherty, M. Mateescu, A.S. Patel, K. Wade, S. Kimura, L.W. Gonzales, S. Guttentag, P.L. Ballard, M. Koval, Developmental regulation of claudin localization by fetal alveolar epithelial cells, Am. J. Physiol. Lung Cell. Mol. Physiol. 287 (2004) L1266–L1273.
[17] A. Ikari, T. Sato, R. Watanabe, Y. Yamazaki, J. Sugatani, Increase in claudin-2 expression by an EGFR/MEK/ERK/c-Fos pathway in lung adenocarcinoma A549 cells, Biochim. Biophys. Acta 1823 (2012) 1110–1118.
[18] T. Sourisseau, A. Georgiadis, A. Tsapara, R.R. Ali, R. Pestell, K. Matter, M.S. Balda, Regulation of PCNA and cyclin D1 expression and epithelial morphogenesis by the ZO-1-regulated transcription factor ZONAB/DbpA, Mol. Cell. Biol. 26 (2006) 2387–2398.
[19] M. Yasen, K. Kajino, S. Kano, H. Tobita, J. Yamamoto, T. Uchiumi, S. Kon, M. Maeda, G. Obulhasim, S. Arii, O. Hino, The up-regulation of Y-box binding proteins (DNA binding protein A and Y-box binding protein-1) as prognostic markers of hepatocellular carcinoma, Clin. Cancer Res. 11 (2005) 7354–7361.
[20] T. Nakatsura, S. Senju, K. Yamada, T. Jotsuka, M. Ogawa, Y. Nishimura, Gene cloning of immunogenic antigens overexpressed in pancreatic cancer, Biochem. Biophys. Res. Commun. 281 (2001) 936–944.
[21] M. Buchert, M. Papin, C. Bonnans, C. Darido, W.S. Raye, V. Garambois, A. Pelegrin, J.F. Bourgaux, J. Pannequin, D. Joubert, F. Hollande, Symplekin promotes tumorigenicity by up-regulating claudin-2 expression, Proc. Natl. Acad. Sci. U. S. A. 107 (2010) 2628–2633.
[22] A. Ikari, T. Sato, A. Takiguchi, K. Atomi, Y. Yamazaki, J. Sugatani, Claudin-2 knockdown decreases matrix metalloproteinase-9 activity and cell migration via suppression of nuclear Sp1 in A549 cells, Life Sci. 88 (2011) 628–633.
[23] J. Bloom, F.R. Cross, Multiple levels of cyclin specificity in cell-cycle control, Nat. Rev. Mol. Cell Biol. 8 (2007) 149–160.
[24] M. Malumbres, M. Barbacid, Cell cycle kinases in cancer, Curr. Opin. Genet. Dev. 17 (2007) 60–65.
[25] H. Huang, Y.D. Hu, N. Li, Y. Zhu, Inhibition of tumor growth and metastasis by non-small cell lung cancer cells transfected with cyclin D1-targeted siRNA, Oligonucleotides 19 (2009) 151–162.
[26] G. Krause, L. Winkler, S.L. Mueller, R.F. Haseloff, J. Piontek, I.E. Blasig, Structure and function of claudins, Biochim. Biophys. Acta 1778 (2008) 631–645.
[27] C.M. Van Itallie, A.J. Tietgens, K. LoGrande, A. Aponte, M. Gucek, J.M. Anderson, Phosphorylation of claudin-2 on serine 208 promotes membrane retention and reduces trafficking to lysosomes, J. Cell Sci. 125 (2012) 4902–4912.
[28] P. Dhawan, R. Ahmad, R. Chaturvedi, J.J. Smith, R. Midha, M.K. Mittal, M. Krishnan, X. Chen, S. Eschrich, T.J. Yeatman, R.C. Harris, M.K. Washington, K.T. Wilson, R.D. Beauchamp, A.B. Singh, Claudin-2 expression increases tumorigenicity of colon cancer cells: role of epidermal growth factor receptor activation, Oncogene 30 (2011) 3234–3247.
[29] S. Xin, C. Huixin, S. Benchang, B. Aiping, W. Jinhui, L. Xiaoyan, W.B. Yu, C. Minhu, Expression of Cdx2 and claudin-2 in the multistage tissue of gastric carcinogenesis, Oncology 73 (2007) 357–365.
[30] S. Tabaries, F. Dupuy, Z. Dong, A. Monast, M.G. Annis, J. Spicer, L.E. Ferri, A. Omeroglu, M. Basik, E. Amir, M. Clemons, P.M. Siegel, Claudin-2 promotes breast cancer liver metastasis by facilitating tumor cell interactions with hepatocytes, Mol. Cell. Biol. 32 (2012) 2979–2991.
[31] G. Sobel, C. Paska, I. Szabo, A. Kiss, A. Kadar, Z. Schaff, Increased expression of claudins in cervical squamous intraepithelial neoplasia and invasive carcinoma, Hum. Pathol. 36 (2005) 162–169.
[32] T.H. Kim, J.H. Huh, S. Lee, H. Kang, G.I. Kim, H.J. An, Down-regulation of claudin-2 in breast carcinomas is associated with advanced disease, Histopathology 53 (2008) 48–55.

[33] P. Vare, I. Loikkanen, P. Hirvikoski, M.H. Vaarala, Y. Soini, Low claudin expression is associated with high Gleason grade in prostate adenocarcinoma, Oncol. Rep. 19 (2008) 25–31.
[34] M.S. Balda, K. Matter, The tight junction protein ZO-1 and an interacting transcription factor regulate ErbB-2 expression, EMBO J. 19 (2000) 2024–2033.
[35] M.S. Balda, M.D. Garrett, K. Matter, The ZO-1-associated Y-box factor ZONAB regulates epithelial cell proliferation and cell density, J. Cell Biol. 160 (2003) 423–432.
[36] S. Islas, J. Vega, L. Ponce, L. Gonzalez-Mariscal, Nuclear localization of the tight junction protein ZO-2 in epithelial cells, Exp. Cell Res. 274 (2002) 138–148.
[37] C.J. Gottardi, M. Arpin, A.S. Fanning, D. Louvard, The junction-associated protein, zonula occludens-1, localizes to the nucleus before the maturation and during the remodeling of cell–cell contacts, Proc. Natl. Acad. Sci. U. S. A. 93 (1996) 10779–10784.
[38] J.W. Lee, W.T. Hsiao, H.Y. Chen, L.P. Hsu, P.R. Chen, M.D. Lin, S.J. Chiu, W.L. Shih, Y.C. Hsu, Upregulated claudin-1 expression confers resistance to cell death of nasopharyngeal carcinoma cells, Int. J. Cancer 126 (2010) 1353–1366.
[39] A. Marchetti, C. Doglioni, M. Barbareschi, F. Buttitta, S. Pellegrini, P. Gaeta, R. La Rocca, G. Merlo, A. Chella, C.A. Angeletti, P. Dalla Palma, G. Bevilacqua, Cyclin D1 and retinoblastoma susceptibility gene alterations in non-small cell lung cancer, Int. J. Cancer 75 (1998) 187–192.
[40] H. Yamanouchi, M. Furihata, J. Fujita, H. Murakami, T. Yoshinouchi, J. Takahara, Y. Ohtsuki, Expression of cyclin E and cyclin D1 in non-small cell lung cancers, Lung Cancer 31 (2001) 3–8.
[41] Y. Guo, K. Yang, J. Harwalkar, J.M. Nye, D.R. Mason, M.D. Garrett, M. Hitomi, D.W. Stacey, Phosphorylation of cyclin D1 at Thr 286 during S phase leads to its proteasomal degradation and allows efficient DNA synthesis, Oncogene 24 (2005) 2599–2612.
[42] V. Baldin, J. Lukas, M.J. Marcote, M. Pagano, G. Draetta, Cyclin D1 is a nuclear protein required for cell cycle progression in G1, Genes Dev. 7 (1993) 812–821.
[43] A. Lange, R.E. Mills, C.J. Lange, M. Stewart, S.E. Devine, A.H. Corbett, Classical nuclear localization signals: definition, function, and interaction with importin alpha, J. Biol. Chem. 282 (2007) 5101–5105.